ACCURACY AND PRECISION OF ALGORITHMS TO DETERMINE THE EXTENT OF AQUATIC PLANTS: EMPIRICAL SCALING OF SPECTRAL INDICES VS. SPECTRAL UNMIXING

E. Cheruiyot[1,2], M. Menenti[1], B. Gorte[1], C. Mito[2] and R. Koenders[1]

[1]*Department of Geoscience and Remote Sensing, Delft University of Technology, P.O. Box 5048, 2600 GA Delft, The Netherlands, Email: E.K.Cheruiyot@tudelft.nl*

[2]*Department of Physics, University of Nairobi, P.O. Box 30197, 00100 Nairobi, Kenya, Email; kipcheru@yahoo.com*

ABSTRACT

Assessing the accuracy of image classification results is an important but often neglected step. Accuracy information is necessary in assessing the reliability of map products, hence neglecting this step renders the products unusable. With a classified Landsat-7 TM image as reference, we assessed the accuracy of NDVI and linear spectral unmixing (LSU) in vegetation detection from 20 randomly selected MERIS sample pixels in the Winam Gulf section of Lake Victoria. We noted that though easy to compute, empirical scaling of NDVI is not suitable for quantitative estimation of vegetation cover as it is misleading and often omits useful information. LSU performed at 87% based on RMSE. For quick solutions, we propose the use of a conversion factor from NDVI to vegetation fractional abundance (FA). With this conversion which is 96% reliable, the resulting FA from our samples were classified at 84% accuracy, only 3% less than those directly computed using LSU.

1. INTRODUCTION

The need for improved satellite data and information extraction methods for global land cover mapping cannot be overemphasised. Accuracy assessment is a critical part of the quality assurance procedure (Latifovic & Olthof, 2004), and it is therefore essential that researchers and users of remotely sensed data have a strong knowledge of both the factors needed to be considered as well as the techniques used in performing any accuracy assessment (Congalton, 1991).

When estimating the extent of aquatic vegetation cover, accurate mapping is important for two reasons. First, an accurate estimate of vegetation cover in the lake provides reliable information to the lake management authorities used to aid in decision making particularly with regard to vegetation control. Second, the information also improves the quality of related studies which rely on vegetation cover estimates for their analyses.

Researchers have responded by applying various techniques to map aquatic vegetation and to quantify the extent of its cover. These include, among others, empirical scaling of NDVI (Ma *et al.* 2008, Fusilli *et al.* 2013) and linear spectral unmixing (Cheruiyot, 2012). Information about the accuracy the maps afforded is not always provided. Therefore the reliability of such products is not guaranteed and the intended user questions their validity.

Both map producers and users benefit from accuracy assessment. To the producers, it is a means through which they communicate product limitations to users, leading to appropriate map use (Latifovic & Olthof, 2004). It also helps them to evaluate and compare the effectiveness of various classification methodologies, ultimately helping to improve their products. To the users, this information is useful in ascertaining the level of reliability of the products. Our research questions are thus; do the methods that have been applied to estimate vegetation cover in inland waters provide accurate results? And how can the accuracy and precision of the algorithms be tested?

Accuracy assessment has greatly evolved over the past three decades since early 1980's, with some of the earliest forms as casual as 'It looks good' (Congalton, 1991). Congalton (1991) provided a summary of all the standard techniques used in accuracy assessment, and noted that the error/confusion matrix has become one of the most commonly used method of classification accuracy assessment. It requires a lot of manual effort to sample and to identify homogeneous regions for the reference pixels. This method also largely relies on the assumption that the reference pixels represent the pure cover components (endmembers) (Asis *et al.* 2008), which may not be the case, especially when the reference pixels are large.

In this study, we assess the accuracy and precision of two algorithms: empirical scaling of spectral indices

Proc. 'ESA Living Planet Symposium 2013', Edinburgh, UK 9–13 September 2013 (ESA SP-722, December 2013)

(NDVI) and linear spectral unmixing in estimation of vegetation cover in the lake. We assess classification by performing correlation between the classified results and the reference data. Here, we use as our reference data the classification results of higher resolution imagery.

2. STUDY AREA

Our study area is Lake Victoria, East Africa in general and Winam Gulf section in particular. It stretches 412 km from north to south between 0° 30' N and 3° 12' S and 355 km from west to east between 31° 37' E and 34° 53' E. The lake, which is the largest of all African lakes, is also the second largest freshwater body in the world, with an extensive surface area of 68 800 km^2. Fig. 1 shows the geographic location of Lake Victoria.

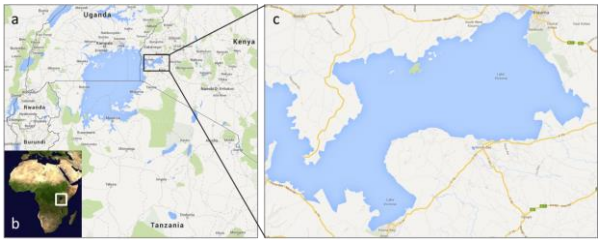

Figure 1. Geographic location of Lake Victoria in East Africa (a) and Africa (b), (c) Zoomed-in Winam Gulf section of the lake

The almost enclosed shallow section of the lake is more vulnerable to vegetation invasion perhaps due to high levels of eutrophication. Earlier work of (Cheruiyot, 2012) and (Fusilli *et al*. 2013) show that vegetation proliferation is preceded by high levels of water quality indicators of eutrophication such as total suspended matter (TSM) by about two months. The most prevalent of these invasive weeds include the non-native water hyacinth and hippo-grass. The weeds are associated with many adverse effects which include obstruction to fishing, navigation and irrigation, interference with the aquatic biodiversity, water quality deterioration and a general risk to public health (Mailu *et al*. 2000, Albright *et al*. 2004). The lake is an important economic resource to the three riparian countries, Kenya Tanzania and Uganda through fishing and transport, as well as providing a livelihood for the local communities.

3. MATERIALS AND METHOD

3.1 Data

We test the performance of the algorithms in estimating vegetation cover with medium resolution imagery by comparing them with higher resolution imagery. The medium resolution imagery used is MERIS FR (full resolution mode), while the high resolution imagery used for validation is Landsat-7. The specifications of this data is summarised in Tab. 1.

Table 1. A summary of satellite data used in the study

Sensor	Date of acquisition	Spatial resolution	Spectral resolution (Visible and NIR)
MERIS FR	15 Dec 2010	300 m	15 bands
Landsat-7 TM	15 Dec 2010	30 m	5 bands

The other data required for this study includes spectral measurements of some endmembers for use in classification. Here, we use the spectral library for Lake Victoria developed by (Cheruiyot, 2012). This library was developed following a field campaign conducted in Lake Victoria in December 2010. Fig. 2 shows a compiled spectral endmember library that was used for classification in this study for MERIS images, while Fig. 3 is a compiled spectral endmember library for Landsat-7 images.

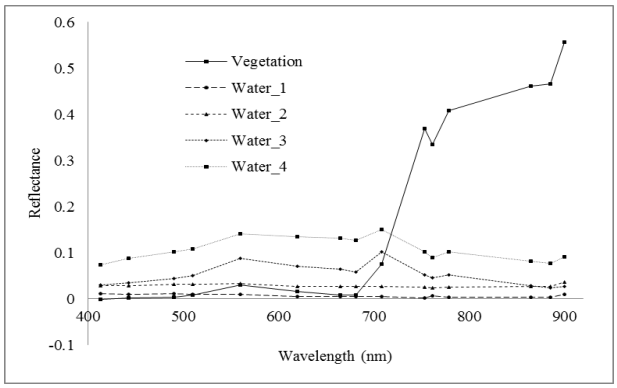

Figure 2. The MERIS endmember spectral library used in classification

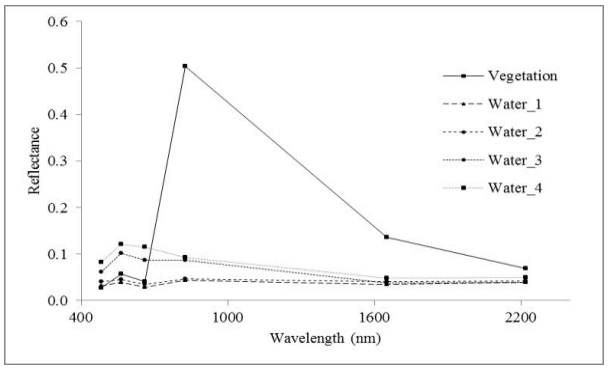

Figure 3. The Landsat-7 endmember spectral library used in classification

3.2 Pre-processing

To use the satellite data, we convert the sensor radiance values into reflectance values and perform atmospheric corrections. Atmospheric corrections of MERIS data were performed using SMAC Processor 1.5.203 (a Simplified Method for Atmospheric Corrections of satellite measurements) (Rahman & Dedieu, 1994), incorporated in the software package BEAM (Basic ERS & Envisat (A) ATSR and Meris Toolbox). It is a semi-empirical approximation of the radiative transfer in the atmosphere which takes into account the attenuation due to atmospheric absorption and radiance of the scattered skylight. We used FLAASH (Fast Line-of-sight Atmospheric Analysis of Spectral Hypercubes), an atmospheric correction code based on the MODTRAN 4 (MODerate resolution atmospheric TRANsmission) radiative transfer model, to convert Landsat TM sensor radiance to apparent reflectance.

3.1 Empirical scaling of spectral indices

Normalized Difference Vegetation Index (NDVI) (Rouse *et al*. 1974 & Deering, 1978) is a dimensionless quantity which is an indicator of the greenness of vegetation in a scene, and is based on the contrast between the maximum reflection in the near infrared (NIR) caused by leaf cellular structure and the maximum absorption in the red (R) due to chlorophyll pigments (Haboudane *et al.* 2004). It is expressed as a ratio of the difference and the sum of NIR and R bands:

$$NDVI = \frac{NIR - R}{NIR + R} \tag{1}$$

Among the many vegetation indices that exist (Jackson & Huete, 1991), Viña *et al.* 2011), NDVI is the most commonly used indicator of vegetation parameters in remotely sensed data (Elmore *et al.* 2000, Haboudane *et al.* 2004) for global vegetation mapping. Though NDVI is not designed to compute the spatial extent of vegetation in a scene, it has been applied to estimate the vegetation cover in various studies, both terrestrial (Lunetta *et al.* 2006), Xiaoxia *et al.* 2008) as well as aquatic (Ma *et al.* 2008, Fusilli *et al*. 2013). When applied in this sense, a means to convert NDVI values into areal estimates must be established. Empirical scaling of spectral indices is commonly used. The challenge, however, is the accuracy in determining thresholds separating the various feature classes in the scene. Fusilli *et al*. (2013) estimated the aquatic vegetation cover in Lake Victoria using the scaling:

$$NDVI = \begin{cases} > 0.4 & Floating\ vegetation \\ 0.2 - 0.4 & Sub - merged\ vegetation \\ < 0.2 & Open\ water\ surface \end{cases} \tag{2}$$

3.2 Linear spectral unmixing (LSU)

Linear Spectral Unmixing (LSU) is a supervised classification technique which is based on the assumption that the observed reflectance of a pixel at any given wavelength band is a linear combination of the reflectance of several individual class features represented in that pixel at that wavelength, and the contribution of each depends on its respective abundance. Therefore the reflectance, R_k of a pixel at wavelength *k* can be expressed as;

$$R_k = \sum_{i=1}^{n} a_i \cdot E_{i,k} + \varepsilon_k \tag{3}$$

$E_{i,k}$ is reflectance of endmember *i* at wavelength *k*, a_i is the abundance of endmember *i*, n is the number of endmembers, and ε_k is the residual error at wavelength *k*. For proper functioning of the model, two conditions are introduced; the sum to one condition, Eq. 4, and positivity condition, Eq. 5.

$$\sum_{i=1}^{n} a_i = 1 \tag{4}$$

$$0 < a_i < 1 \tag{5}$$

A constrained model is one which applies any of these two conditions. A model operating with both conditions is said to be fully constraint, while an unconstraint model operates without any condition. The number of spectral bands in an image introduces a limitation to the number of endmembers that can be used for unmixing (Theseira *et al.* 2002), so that it must always be less than the number of available bands in the multispectral image, m:

$$n < m \tag{6}$$

LSU is one of the Spectral Mixture Analysis (SMA) techniques which are used to decompose a mixed pixel into various distinct components. It is most suitable where the spatial resolution of the satellite data is relatively course. It has been applied in various researches which include analysis of rock and soil types (Adams & Smith, 1986), desert vegetation (Smith *et al.* 1990), land-cover changes (Adams *et al.* 1995), estimation of urban vegetation abundance (Small, 2001 & Small, 2003), and delineating potential erosion areas in tropical watersheds (Asis *et al.* 2008). Non-linear mixture models also exist (Liu & Wu, 2005), but LSU is by far the most common type of SMA, and is widely used because of its simplicity and interpretability (Asis *et al.* 2008).

3.3 Sample Pixels and analysis

We sampled out points within Winam Gulf where classification accuracy would be assessed. We randomly selected 20 sample pixels scattered within the Winam Gulf from MERIS and export them to Landsat, where the corresponding Landsat-7 pixels were identified. One MERIS pixel corresponds to 10 by 10 Landsat-7 pixels. Fig. 4 shows these sample points. Fig. 4(a) shows the sample pixels labeled M1 – M20, 4(b) is a zoomed-in MERIS pixel, while 4(c) shows the corresponding 100 Landsat-7 pixels. With the 300 m spatial resolution MERIS imagery, we use as our reference data the 30 m spatial resolution Landsat-7 imagery for accuracy and precision determination of both NDVI scaling and LSU classification methods.

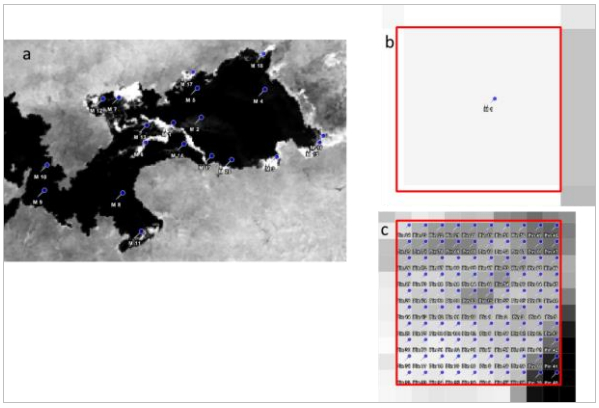

Figure 4. (a) Location of the 20 randomly selected sample pixels, (b) M1 MERIS pixel (300 m), (c) Corresponding 100 Landsat TM pixels (30 m)

We apply the NDVI scaling in Eq. 2 to assess accuracy and precision of NDVI in vegetation estimation from the selected sample pixels. NDVI was computed from Landsat TM using band 3 and band 4, centered at 660 nm and 825 nm, for R and NIR respectively. For MERIS NDVI, we used bands 7 and 13, centered at 664 nm and 865 nm, for R and NIR respectively. These two pairs of R and NIR are the closest we could obtain from MERIS and Landsat TM.

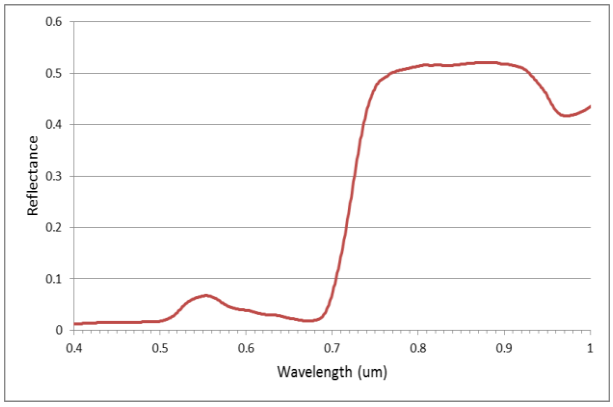

Figure 5. Field measurement of water hyacinth spectrum

Using different values of R and NIR for the two datasets inevitably lead to some difference in computed NDVI from the two images. With *in-situ* spectral measurements of water hyacinth shown in Fig. 5, we assessed the effect of this difference, and found that it's magnitude is in the order of NDVI = 0.005, which is too small to cause any significant impact on our results. For Landsat TM, we first obtained the mean reflectance of band 3 and band 4 from the 100 pixels before using them to compute NDVI value corresponding to one MERIS pixel. This is because NDVI is a non-linear parameter, and mean NDVI cannot be computed directly.

With exactly the same 20 sample pixels as were used for the NDVI accuracy assessment, we apply a fully constrained LSU with five endmembers to assess accuracy and precision of spectral unmixing in vegetation estimation. The five endmembers are four water classes at varying eutrophication levels and one vegetation class (see endmember spectral libraries shown in Fig. 2 and 3). These are the predominant feature classes in the image, identified following an unsupervised classification (Cheruiyot, 2012).

4. RESULTS AND DISCUSSION

We assess the scaling of NDVI for the 20 randomly selected sample pixels M1 – M20 following the work of Fusilli *et al.* (2013), where NDVI scaling given in Eq. 2 was used. Tab. 2 is a summary of this analysis. The

'NDVI' column shows NDVI value of the 100 pixels corresponding to the one sample MERIS pixel, while 'Classification' column gives an appropriate classification of that NDVI value according to the NDVI scaling of Eq. 2. The next three columns provide the distribution of the 100 Landsat-7 according to their NDVI values to the three classes of Eq. 2; 'Floating vegetation' (FV), 'Submerged vegetation' (SV) and 'Open water' (OW).

Table 2. A summary of the NDVI scaling of some selected sample pixels

Sample Pixel	NDVI	Classification	FV	SV	OW
M1	0.64	FV	97	1	2
M2	0.19	OW	11	28	61
M3	0.85	FV	100	0	0
M4	0.04	OW	0	0	100
M11	0.36	SV	42	10	48
M12	0.38	SV	40	7	53
M18	0.43	FV	42	13	45
M19	0.27	OW	27	4	69

The table shows NDVI computed from mean band 3 and band 4 reflectance of 100 subpixels for each sample pixel, and an appropriate classification following NDVI scaling of Eq. 2. A closer look at these results reveals serious classification issues. M11, for instance, has a mean NDVI of 0.36, which effectively places it in SV category. However, only 10% of the reference pixels actually fall in this category, while the other 90% are in the other two categories. By classifying M11 as SV, one treats all 42 FV pixels and 48 OW pixels as if they were all SV pixels. Similarly, 27 pixels of FV in M19 are completely ignored in vegetation cover estimation, since the average NDVI places it as OW. This shows that scaling of NDVI can be misleading along the border of two distinct endmembers. Quantitatively, there are 9 out of 20 sample pixels classified as FV, which gives vegetation abundance of 0.45. With the mean vegetation abundance of these 20 pixels from the reference data being 0.3, then this estimation is only 50% accurate.

A comparison was made for fractional abundance of vegetation as derived by LSU from MERIS imagery and from the reference data, Landsat-7 TM (see Fig. 6). It is seen here that MERIS image was classified with an accuracy of 87% (R^2 = 0.78 and RMSE = 0.13) with Landsat-7 as reference.

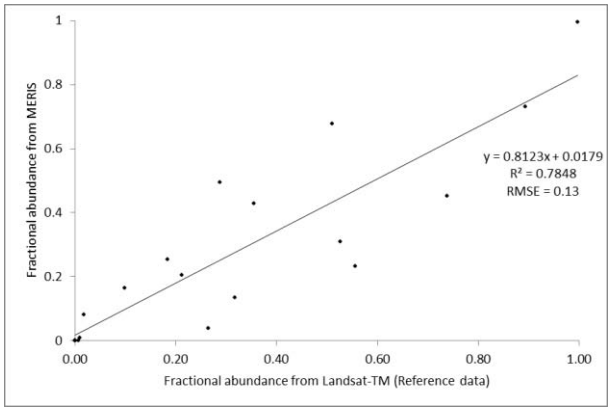

Figure 6. A scatter plot showing a correlation between vegetation fractional abundance values obtained from a MERIS pixel and the corresponding mean fractional abundance values obtained from Landsat-7 pixels over the same scene

In this case LSU performs 37% better than NDVI in estimating vegetation cover. Computation of LSU requires a good compilation of endmembers in addition to the satellite imagery. Performance of LSU largely depends on the quality of the selection of endmembers. On the contrary, scaling of NDVI is easy to compute as one needs no ancillary data other than the NIR and red bands from the imagery. However, NDVI does not directly provide areal vegetation cover estimates. We explore relationship between fractional abundance and NDVI provided in Fig. 7 to establish a conversion factor from NDVI to FA, which could be used to more easily estimate actual vegetation cover.

Fig. 7 shows a relationship between NDVI and fractional abundance over the lake area, both derived from the same image. The relationship is non-linear, an indication that NDVI should not be used to directly estimate areal cover of vegetation. While FA is a linear parameter, NDVI is not. It saturates at high levels of vegetation density especially from NDVI = 0.7, so that any further increase in vegetation does not give a proportionate increase in NDVI.

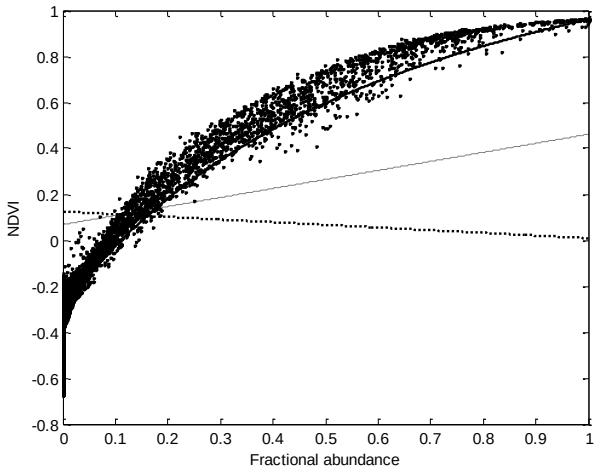

Figure 7. The horizontal axis is vegetation abundance, FA (= 1 - water abundance). The dotted line is the red (R) band, assumed to go down linearly from 0.12 (pure water) to 0.01 (pure vegetation). Dashed line is NIR, going up from 0.07 to 0.46. The solid curve is NDVI = (NIR – R) / (NIR + R), and the dots are the computed FA vs. NDVI for all pixels inside the shoreline

We obtain an equation that best describes the curve of Fig. 7. We did this by selecting two pixels that we identified as being homogeneous; one with pure vegetation and the other with pure water and obtained their R and NIR values. Assuming linearity, we obtained the rate of their change over the vegetation abundance from 0 to 1, as shown in Fig. 8.

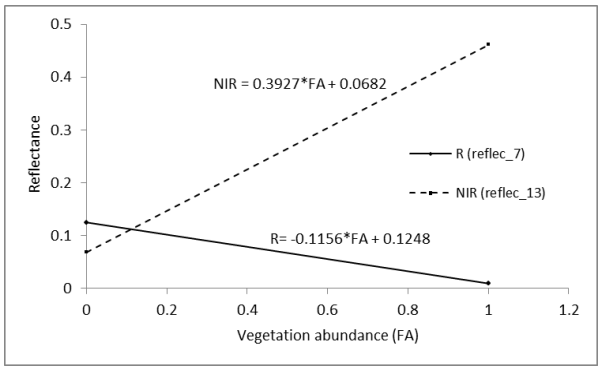

Figure 8. The equations describing the rate of change of R and NIR values between pure water and pure vegetation pixels

Substituting the gradient equations of R and NIR in Fig. 8 into the NDVI Eq. 1 gives the relationship between vegetation abundance (FA) and NDVI;

$$NDVI = \frac{(0.5083 \cdot FA - 0.0566)}{(0.2771 \cdot FA + 0.193)} \qquad (7)$$

Solving for FA, Eq. 7 becomes;

$$FA = \frac{(0.193 \cdot NDVI + 0.0566)}{0.5083 - 0.2771 \cdot NDVI} \qquad (8)$$

The solid line in Fig. 7 corresponds to Eq. 8. With this relationship, we can easily convert NDVI value to its corresponding vegetation FA value for any pixel within the lake. We tested the reliability of this relationship with Landsat TM data, by comparing FA as computed directly from Landsat TM data to FA obtained by converting Landsat TM NDVI using Eq. 8. As shown in Fig. 9, these two sets of FA correlates with $R^2 = 0.9771$ (and RMSE = 0.04), which shows 96% reliability of the conversion Eq. 8 from NDVI to FA.

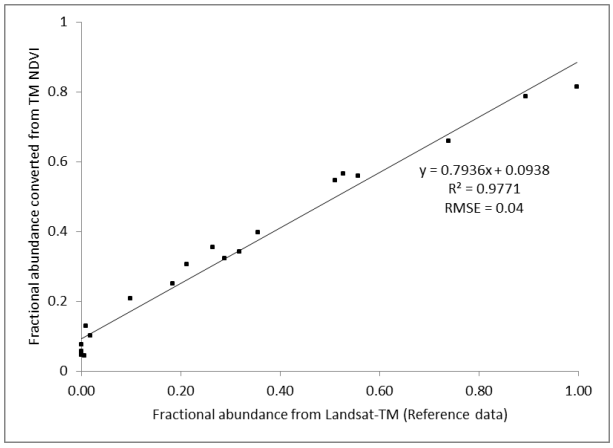

Figure 9. A scatter plot showing a correlation between vegetation FA as computed from a Landsat TM and the corresponding FA obtained by converting Landsat TM NDVI values

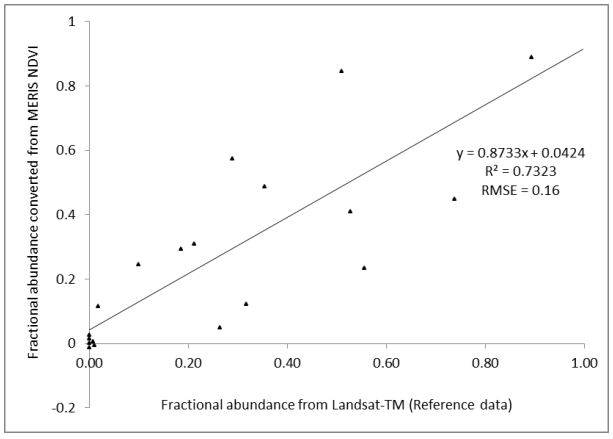

Figure 10. A scatter plot showing a correlation between vegetation FA values obtained from a MERIS pixel and

the corresponding FA values obtained by converting NDVI values over the same pixels

Using Eq. 8, we converted MERIS NDVI to the corresponding vegetation abundances. We tested the accuracy of the resulting vegetation abundance values as compared with our reference data, Landsat TM vegetation fractional abundances (see Fig. 10). It is observed here that the converted FA values were classified at $R^2 = 0.73$ (and RMSE = 0.16) which shows 84% accuracy.

Results of Fig. 6 and 10 reveal that LSU performs better than NDVI by about 3%. One reason is that the conversion factor of Eq. 8 is not entirely perfect, and the other is that LSU makes use of many bands in computing the fractional abundances, while NDVI is limited to only two. Even though it is not easy to tell the contribution of each of the extra band to the overall accuracy of LSU, the increased spectral dimensionality certainly improves the detection of vegetation and discrimination from other feature classes. The difference of 3% in accuracy obtained by the two approaches; directly computing FA using LSU and converting NDVI to FA, is however small compared to the difference in ease and technicality involved in computing them.

5. CONCLUSIONS AND RECOMMENDATIONS

We have examined the performance of LSU and NDVI in vegetation detection and vegetation area estimation. Using a classified 30 m spatial resolution Landsat-7 TM as our reference data, we tested the performance of NDVI as well as LSU in detecting vegetation from a 300 m spatial resolution MERIS imagery. Results reveal that scaling of NDVI may produce biased results when dealing with inhomogeneous regions as it assigns the entire pixel to one of the available class features. Consequently, some information in the pixel contributed by the other features that were not selected is entirely ignored. We therefore find scaling of NDVI quite inaccurate and unreliable for quantitative analysis of heterogeneous surfaces. On the other hand, LSU decomposes the pixel into various class features according to their relative abundances, and no information is discarded. Compared to the reference data, LSU with five endmembers classified MERIS image at 87% accuracy.

Despite the limitations of empirical scaling of NDVI in vegetation area estimation, it is a lot easier to compute NDVI as it requires no ancillary data unlike LSU which requires, in addition to multispectral image, a well-defined endmember spectral library. Besides, one requires other ancillary data to perform atmospheric corrections to the image before applying LSU. We have proposed a relationship that could be used to convert pixel NDVI values to pixel vegetation FA values in our study area of aquatic vegetation. The conversion relationship of NDVI to FA is 96% reliable, i.e. the converted FA compares to the directly computed FA by $R^2 = 0.9771$. Application of this conversion to MERIS NDVI produced vegetation FA which is 84% accurate compared to the reference data. This is only about 3% less accurate than what would be obtained by directly computing FA using LSU. The relationship may vary for various applications such as for terrestrial and aquatic environments.

ACKNOWLEDGEMENTS

This research was carried out under the framework of ESA's (European Space Agency) ALCANTARA Initiative, and was facilitated by Delft University of Technology, The Netherlands, and the University of Nairobi, Kenya.

REFERENCES

Adams, J. B., & Smith, M. O. (1986). Spectral Mixture Modeling: A New Analysis of Rock and Soil Types at the Viking Lander 1 Site. *Journal of Geophysical Research, 91*(B8), 8098-8112.

Adams, J. B., Sabol, D. E., Kapos, V., Filho, R. A., Roberts, D. A., Smith, M. O., & Gillespie, A. R. (1995). Classification of Multispectral Images Based on Fractions of Endmembers: Application to Land-Cover Change in the Brazilian Amazon. *Remote Sensing of Environment, 52*, 137-154.

Albright, T. P., Moorhouse, T. G., & McNabb, T. J. (2004). The rise and fall of water hyacinth in Lake Victoria and the Kagera River basin, 1989-2001. *Journal of Aquatic Plant Management, 42*, 73-84.

Asis, A. D., Omasa, K., Oki, K., & Shimizu, Y. (2008). Accuracy and applicability of linear spectral unmixing in delineating potential erosion areas in tropical watersheds. *International Journal of Remote Sensing, 29*(14), 4151-4171.

Cheruiyot, E. K. (2012). *Monitoring aquatic plants proliferation in Lake Victoria using satelitte data.* University of Nairobi. Nairobi: University of Nairobi Press.

Congalton, R. G. (1991). A Review of Assessing the Accuracy of Classifications of Remotely Sensed Data. *Remote Sensing of Environment, 37*, 35-46.

Deering, D. W. (1978). *Rangeland reflectance characteristics measured by aircraft and spacecraft sensors.* Texas A & M University. TX: College Station.

Elmore, A. J., Mustard, J. F., Manning, S. J., & Lobell, D. B. (2000). Quantifying vegetation change in semi-arid environment; precision and accuracy of spectral mixture analysis and the Normalized Difference Vegetation Index. *Remote Sensing of Environment, 73*, 87-102.

Fusilli, L., Collins, M. O., Laneve, G., Palombo, A., Pignatti, S., & Santini, F. (2013). Assessment of the abnormal growth of floating macrophytes in Winam Gulf (Kenya) by using MODIS imagery time series. *International Journal of Applied Earth Observation and Geoinformation, 20*, 33-41.

Haboudane, D., Miller, J. R., Pattey, E., Zarco-Tejada, P. J., & Strachan, I. B. (2004). Hyperspectral vegetation indices and novel algorithms for predicting green LAI of crop canopies: Modeling and validation in the context of precision agriculture. *Remote Sensing of Environment, 90*, 337-352.

Jackson, R. D., & Huete, A. R. (1991). Interpreting vegetation indices. *Preventive Veterinary Medicine, 11*, 185-200.

Latifovic, R., & Olthof, I. (2004). Accuracy assessment using sub-pixel fractional error matrices of global land cover products derived from satellite data. *Remote Sensing of Environment, 90*, 153-165.

Liu, W., & Wu, E. Y. (2005). Comparison of non-linear mixture models: sub-pixel classification. *Remote Sensing of Environment, 94*, 145-154.

Lunetta, R. L., Knight, F. K., Ediriwickrema, J., Lyon, J. G., & Worthy, L. D. (2006). Land-cover change detection using multi-temporal MODIS NDVI data. *Remote Sensing of Environment*(105), 142-154.

Ma, R., Duan, H., Gu, X., & Zhang, S. (2008). Detecting Aquatic Vegetation Changes in Taihu Lake, China Using Multi-temporal Satellite Imagery. *Sensors, 8*, 3988-4005. doi:10.3390/ s8063988

Mailu, A. M., Ochiel, G. R., Gitonga, W., & Njoka, S. W. (2000). Water hyacinth: an environmental disaster in the Winam Gulf of Lake Victoria and its control. *Proceedings of the 1st IOBC water hyacinth working group*, (pp. 101-105).

Rahman, H., & Dedieu, G. (1994). SMAC: a simplified method for the atmospheric correction of satellite measurements in the solar spectrum. *International Journal of Remote Sensing, 15*(1), 123-143. doi:DOI: 10.1080/01431169408954055

Rouse, J. W., Haas, R. H., Schell, J. A., Deering, D. W., & Harlan, J. C. (1974). *Monitoring the vernal advancements and retrogradation of natural vegetation.* Greenbelt. MD, USA: NASA/GSFC.

Small, C. (2001). Estimation of urban vegetation abundance by spectral mixture analysis. *International Journal of Remote Sensing, 22*(7), 1305-1334.

Small, C. (2003). High spatial resolution spectral mixture analysis of urban reflectance. *Remote Sensing of Environment, 88*, 170-186.

Smith, M. O., Ustin, S. L., Adams, J. B., & Gillespie, A. R. (1990). Vegetation in Deserts: I. A Regional Measure of Abundance from Multispectral Images. *Remote Sensing of Envrionment, 31*, 1-26.

Theseira, M. A., Thomas, G., & Sannier, C. A. (2002). An evaluation of spectral mixture modelling applied to a semi-arid environment. *Internationa l Journal of Remote Sensing, 23*(4), 687-700.

Viña, A., Gitelson, A. A., Nguy-Robertson, A. L., & Peng, Y. (2011). Comparison of different vegetation indices for the remote assessment of green leaf area index of crops. *Remote Sensing of Environment, 115*(12), 3468-3478.

Xiaoxia, S., Jixian, Z., & Zhengjun, L. (2008). Vegetation cover annual changes based on MODIS/TERRA NDVI in the Three Gorges reservoir area. *The International Archives of the Photogrammetry, Remote Sensing and Spatial Information Sciences, XXXVII*(B7), pp. 1397-1400.